

Mandibular alveolar bone thickness in untreated Class I subjects with different vertical skeletal patterns: a cone-beam computed tomography study

Joseph Formosa^a; Min Zou^b; Chun-Hsi Chung^c; Normand S. Boucher^d; Chenshuang Li^e

ABSTRACT

Objective: To evaluate the mandibular alveolar bone thickness in untreated skeletal Class I subjects with different vertical skeletal patterns.

Materials and Methods: A total of 50 preorthodontic treatment cone-beam computed tomography (CBCT) images of a skeletal Class I Chinese population with near-normal occlusion were selected. The buccal and lingual alveolar bone thicknesses of mandibular canines to second molars were measured at 2 mm below the cemento-enamel junction (CEJ), mid-root, and root apex levels. Differences in the measurements were analyzed with Mann-Whitney *U*-test. The correlation between alveolar bone thickness and the sella-nasion–mandibular plane (SN-MP) angle was calculated using Pearson correlation coefficients and linear regression analysis.

Results: Buccal alveolar bone was thinner on all mandibular canines to first molars but thicker on second molars in comparison with lingual alveolar bone. Buccal alveolar bone was within 1 mm at the levels of 2 mm below CEJ and mid-root for the canines and first premolars. Significant differences were detected among subjects with different vertical patterns, with a negative correlation between the SN-MP angle and alveolar thickness, especially in the canine and premolar regions. The thinnest buccal and lingual alveolar bone were detected in the high-angle group canine region (0.50 mm at the levels of 2 mm below CEJ and mid-root for the buccal side, 0.90 mm at the level of 2 mm below the CEJ for the lingual side).

Conclusions: To avoid periodontal complications, buccal-lingual movement of the mandibular canines and first premolars should be limited, especially in high-angle patients. (*Angle Orthod.* 2023;93:683–694.)

KEY WORDS: Alveolar bone; Skeletal vertical pattern; CBCT; Mandible

^a Former Resident in Periodontic/Orthodontic Postgraduate Program, Department of Orthodontics, School of Dental Medicine, University of Pennsylvania, Philadelphia, Pa, USA.

^b Associate Professor, Department of Orthodontics, Key Laboratory of Shannxi Province for Craniofacial Precision Medicine Research, Clinical Research Center of Shannxi Province for Dental and Maxillofacial Diseases, College of Stomatology, Xi'an Jiaotong University, Xi'an, China.

^c Associate Professor and Chauncey M. F. Egel Endowed Chair and Director, Department of Orthodontics, School of Dental Medicine, University of Pennsylvania, Philadelphia, Pa, USA.

^d Associate Clinical Professor, Department of Orthodontics, School of Dental Medicine, University of Pennsylvania, Philadelphia, Pa, USA.

^e Assistant Professor, Department of Orthodontics, School of Dental Medicine, University of Pennsylvania, Philadelphia, Pa, USA.

Corresponding author: Dr Chenshuang Li, 240 S 40th Street, Philadelphia, PA 19104, USA
(e-mail: lichens@upenn.edu)

Accepted: June 2023. Submitted: March 2023.

Published Online: July 28, 2023

© 2023 by The EH Angle Education and Research Foundation, Inc.

INTRODUCTION

The morphology and size of the mandibular alveolar bone plays a critical role in planning orthodontic treatment. The assessment of periodontal tissue dimensions and the identification of mucogingival risks are important prior to orthodontic treatment as they will influence the esthetic outcome and integrity of the periodontium.¹ Wennström reported that facial/labial tooth movement could reduce the buccolingual thickness of tissue on the facial side, decrease the keratinized gingiva on the facial side, and reduce the facial height of the soft tissue margin.² If teeth are moved beyond the alveolar limit, not only will the treatment result be unstable but also periodontal problems, such as bone dehiscence and gingival recession, will follow.^{2,3} Recently, Allahham et al. evaluated the cone-beam computed tomography (CBCT) images of adult patients with mild-to-moderate crowding treated with nonextraction clear aligner therapy and found an

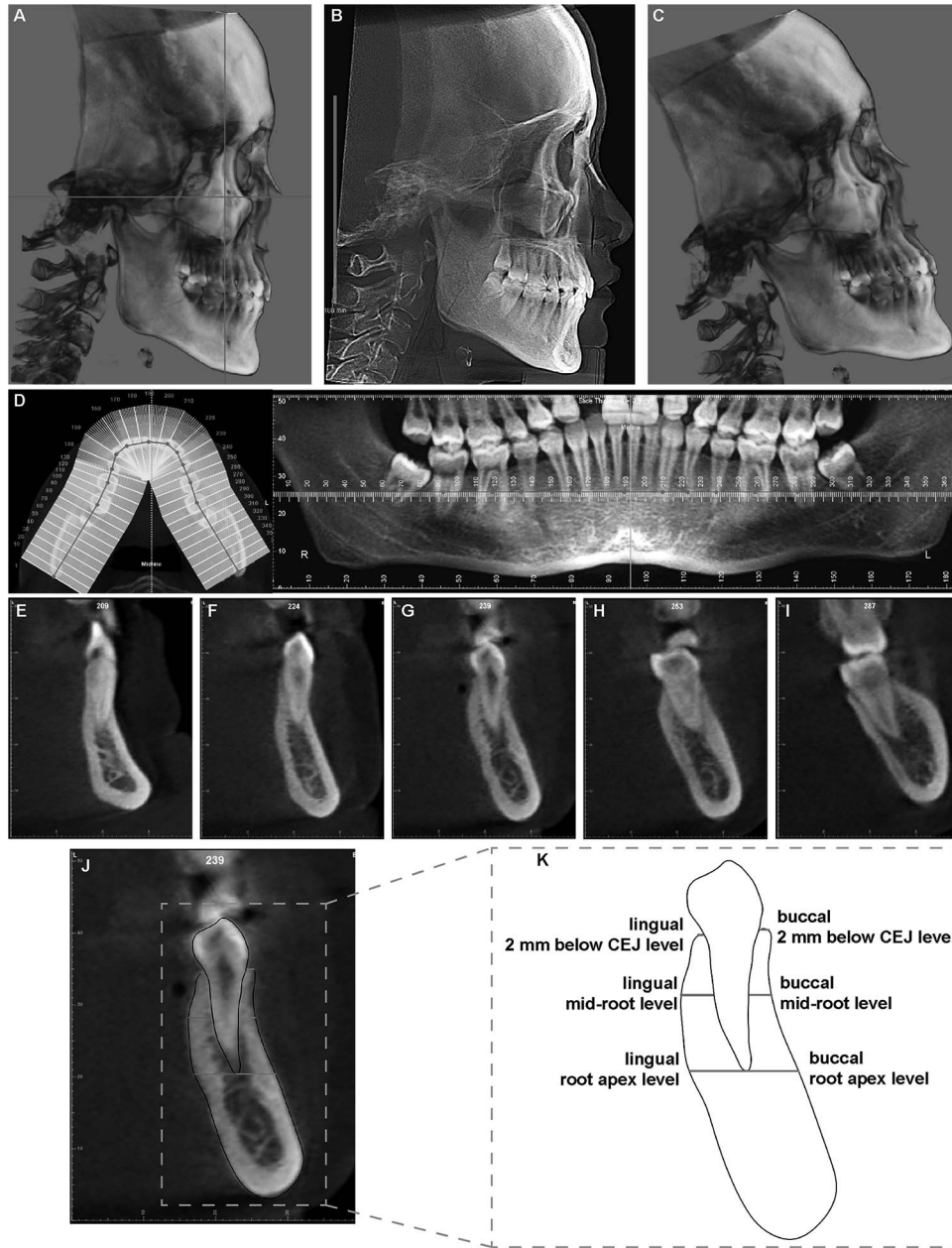


Figure 1. The measurement workflow. (A) The full-cranium cone-beam computed tomography (CBCT) images of each subject were first oriented to Frankfort horizontal plane (horizontal line). (B) Orthogonal (no magnification) lateral cephalometric X-ray was extracted from the CBCT data set for cephalometric analysis. (C) Once the sagittal and vertical skeletal relationships were classified, the CBCT images were then oriented to the anatomical mandibular plane. (D) Using Dolphin three-dimensional software, a CBCT-synthesized panoramic radiograph was generated and used to identify specific coronal slices that represented the long axis of each tooth (E, canine; F, first premolar; G, second premolar; H, first molar; I, second molar). (J, K) Presentation of alveolar bone thickness measurements. CEJ indicates cemento-enamel junction.

increase in alveolar bone dehiscence and fenestration from dental arch expansion.⁴

Clinicians often assess alveolar bone anatomy of the anterior teeth by either subjective palpation or analyzing lateral cephalograms. With the broad adaption of three-dimensional (3D) imaging in the dental field in the past decade, several clinicians/research groups have evaluated alveolar bone thickness in the mandibular incisor

region on CBCT in the past few years and have consistently reported that hyperdivergent patients had a thin symphysis and a thin alveolus in the incisor region.^{5,6}

It is clear in the literature that there is a strong negative correlation between the vertical facial type and mandibular bony support in the mandibular incisors.^{7,8} However, detailed evaluations of buccal and lingual alveolar bone thicknesses in the mandibular posterior

Table 1. Demographic Information of Enrolled Patients in the Current Study^a

| | L | N | H | P Value of <i>t</i> -Test | | |
|-----------------|-------------------------|--------------------------|-------------------------|---------------------------|------------|------------|
| | | | | L vs N | N vs H | L vs H |
| No. of subjects | 16 (9 females, 7 males) | 20 (11 females, 9 males) | 14 (9 females, 5 males) | — | — | — |
| Age (years) | 20.3 ± 2.78 | 24.0 ± 6.77 | 22.2 ± 6.57 | .1366 | .6339 | .6339 |
| ANB (degrees) | 2.51 ± 1.04 | 2.70 ± 1.25 | 2.66 ± 1.27 | .8850 | .9954 | .9365 |
| SN-MP (degrees) | 23.9 ± 2.11 | 33.2 ± 2.89 | 39.9 ± 2.19 | <.0001**** | <.0001**** | <.0001**** |

^a ANB indicates A point–nasion–B point; H, high angle; L, low angle; N, normal angle; and SN-MP, sella-nasion–mandibular plane.
**** *P* ≤ .0001.

region and their relationship with vertical skeletal patterns are lacking. Thus, to provide information on the potential limitation of mandibular dental expansion transversely, the current study aimed to evaluate the mandibular alveolar dimensions of the mandibular canine to the second molar in untreated Class I skeletal subjects using CBCT. In addition, the relationship between the mandibular posterior alveolar bone thickness and vertical facial types was analyzed.

MATERIALS AND METHODS

Patients

The protocol of this study was approved by both the University of Pennsylvania Institutional Review Board (protocol 851249, May 2022) and the College of Stomatology, Xi'an Jiaotong University Medical Ethics Committee (approval xjkqll [2020] NO.014, August 2020). The study was conducted in accordance with the Declaration of Helsinki.

The sample for this retrospective study was recruited from the pretreatment, full-volume CBCT database of Chinese patients seeking orthodontic treatment between 2017 and 2020. The CBCT images were collected from the Department of Orthodontics at College of Stomatology, Xi'an Jiaotong University, which used CBCT imaging as part of the routine preorthodontic records exams. All images were taken using i-Cat (Imaging Sciences International, Hatfield, Pa) at 120 kV, 5 mA, 14 cm × 17 cm field of view, 0.4 mm voxel, and a scan time of 8.9 seconds.⁹ A total of 600 hundred pretreatment, full-volume CBCT images were screened based on the inclusion and exclusion criteria.

The initial screening inclusion criteria were the following: (1) patients 15–40 years of age; (2) permanent dentition with the second molar fully erupted, roots completely formed, minimal dental wear, and < 5 mm anterior crowding or spacing per arch; (3) no missing teeth or supernumerary teeth; (4) canines, premolars, first or second molars all in acceptable occlusion without significant buccolingual displacement or posterior crossbite; and (5) a skeletal Class I with A point–nasion–B point (ANB) angle between 0.7° and 4.7° (based on Chinese cephalometric norms^{10–12}). The initial screening exclusion criteria were (1) craniofacial

syndromes, (2) obvious deformity of the mandible including asymmetry, (3) previous history of craniofacial trauma, (4) history of periodontal disease with significant bone loss, or (5) a history of prior orthodontic therapy.

After initial screening, 102 CBCT images were imported into Dolphin 3D software (version 11.95 premium; Dolphin Imaging, Chatsworth, Calif) and oriented to the Frankfort horizontal plane as previously described (Figure 1A,B).⁹ A second round of screening was performed to exclude the images with posterior periapical defects, posterior impacted teeth (except third molars), or posterior teeth with root canal treatment. After the second round of screening, patients were cataloged into low-, normal-, and high-angle groups based on the Chinese norm of the sella-nasion–mandibular plane (SN-MP) angle (27.3–37.7°).^{10–12}

CBCT Segmentation

Once vertical skeletal relationships were classified, the CBCT images were then oriented to the anatomical mandibular plane using the left and right gonion and right menton (Figure 1C). Using Dolphin 3D software, an axial section of the mandibular arch that allowed identification of the dental canals of the teeth was obtained, and an axial curve was plotted with one point per tooth (the mesial roots for the first and second molars were selected) (Figure 1D). A CBCT-synthesized panoramic radiograph was then used to orient and help identify specific coronal slices (0.5 mm in thickness) that represented the long axis of each tooth (Figure 1E–I).

Table 2. Evaluation of the Measurement System Reliability by Paired *t*-Test and ICC Analysis

| | P Value of Paired <i>t</i> -Test | ICC (Absolute Agreement) [95% CI] ^a |
|-----------------|----------------------------------|--|
| Canine | .090 | 0.986 [0.978, 0.992] |
| First premolar | .125 | 0.987 [0.979, 0.992] |
| Second premolar | .213 | 0.985 [0.976, 0.990] |
| First molar | .862 | 0.979 [0.976, 0.987] |
| Second molar | .114 | 0.988 [0.981, 0.992] |

^a CI indicates confidence interval; ICC, interclass correlation coefficient.

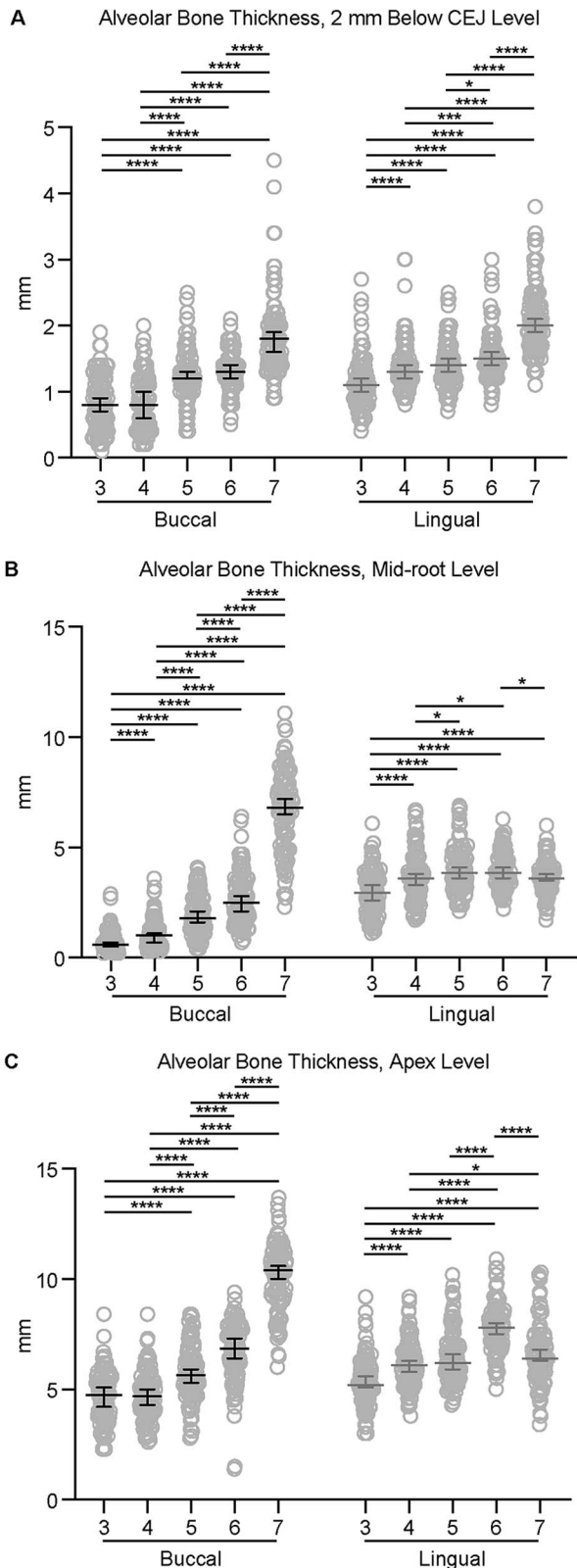


Figure 2. Overview of the alveolar bone thickness of mandibular teeth. Buccal and lingual alveolar bone thickness of mandibular canine, premolar, and molar at (A) the level 2 mm below CEJ, (B) the level of mid-root, and (C) the level of root apex. 3, canine; 4, first premolar; 5, second premolar; 6, first molar; 7, second molar.

Measurements of Alveolar Thickness

On each obtained coronal slice, the following measurements were performed perpendicular to the long axis of each tooth (Figure 1J,K):

- Distance between buccal/lingual cortex to the tooth root surface at the level 2 mm below the cemento-enamel junction (CEJ).
- Distance between buccal/lingual cortex to the tooth root surface at the mid-root level.
- Distance between buccal/lingual cortex to the tooth root surface at the root apex level.

Both the left and right sides were evaluated.

Power Analysis

The sample size was determined based on a power analysis with $\alpha = 0.05$, 80% power, and a Cohen’s d of 1.2, which represents a very large effect size,¹³ to ensure an adequate sample size (minimum of 13 samples per group) for showing statistical differences.

Statistical Analysis

In this study, one trained researcher (Dr Formosa) made all the measurements. The intraoperator error was obtained by repeating measurements by the same observer (Dr Formosa) 1 week apart on 6 randomly selected CBCT files. The intraclass correlation coefficients (ICCs) of the measurements and paired *t*-tests were calculated using the IBM SPSS software (Statistical Package for Social Sciences version 26.0, Chicago, Ill) to test the measurement system reliability.

A Shapiro-Wilk normality test was performed by GraphPad Prism (version 8.2.1; GraphPad Software, San Diego, Calif). For demographic data comparison, analysis of variance was performed and followed by an independent *t*-test. For the alveolar bone thickness comparison, because some of the data did not pass the normal distribution test, data were presented as raw data overlapped with median \pm 95% confidence interval, and the Mann-Whitney *U*-test was used for statistical comparison. Pearson’s correlation coefficient (*r*) calculation and linear regression analysis were also performed by GraphPad Prism.

← Data are presented as raw data overlapped with median \pm 95% confidence interval. * $P \leq .05$; *** $P \leq .001$; **** $P \leq .0001$. CEJ indicates cemento-enamel junction.

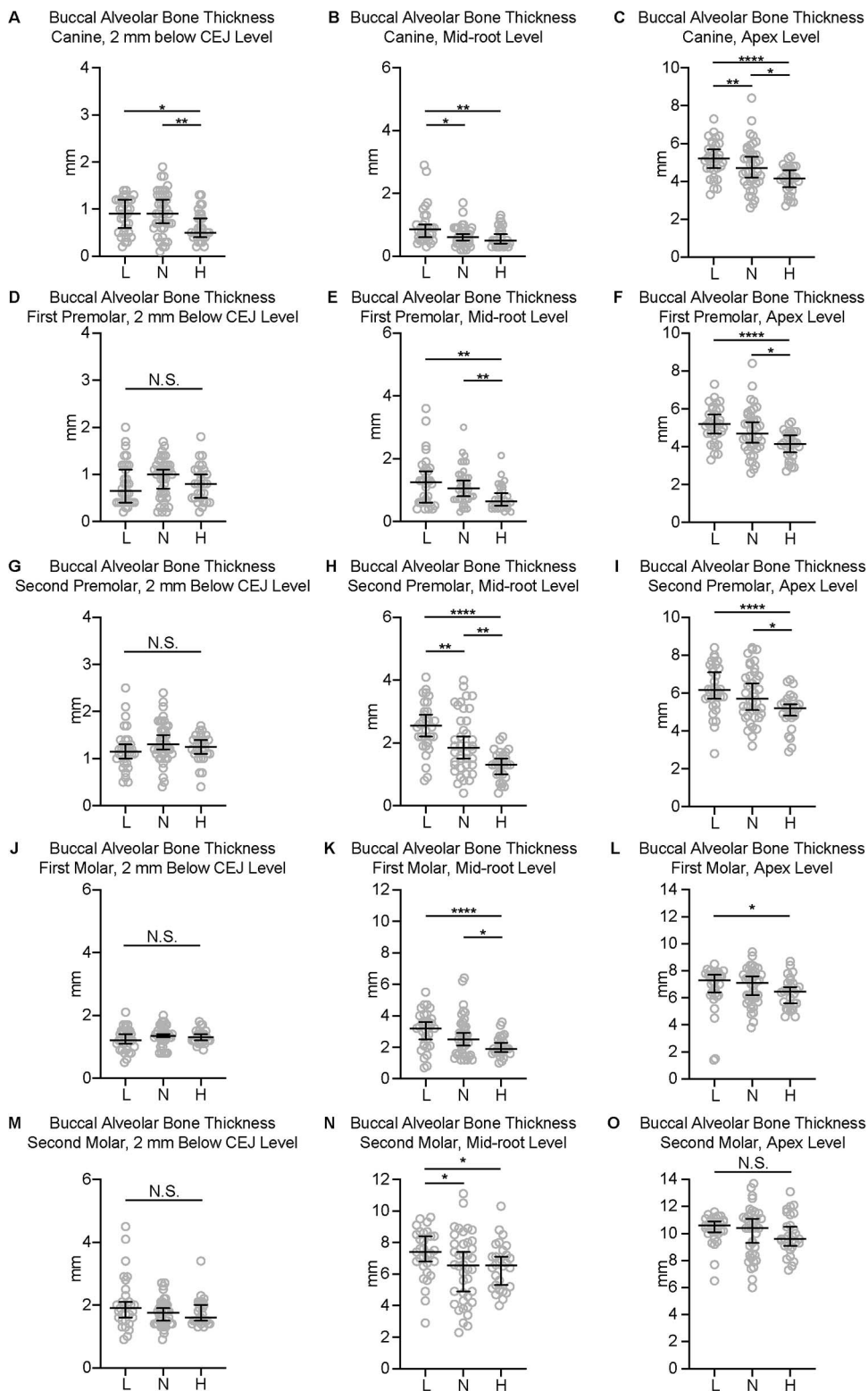


Figure 3. Buccal alveolar bone thickness of mandibular teeth. Buccal alveolar bone thickness of (A–C) canine, (D–F) first premolar, (G–I) second premolar, (J–L) first molar, and (M–O) second molar. Data are presented as raw data overlapped with median ± 95% confidence interval. * $P \leq .05$; ** $P \leq .01$; **** $P \leq .0001$. CEJ indicates cemento-enamel junction; H, high angle; L, low angle; N, normal angle; and N.S., not statistically significant.

Table 4. Buccal Alveolar Bone Thickness of Mandibular Canine to Second Molar^a

| | Buccal Alveolar Bone Thickness, Median [Minimum, Maximum], mm | | | P Value of Mann-Whitney U-Test | | |
|------------------------|--|---------------------|--------------------|--------------------------------|---------|------------|
| | L | N | H | L vs N | N vs H | L vs H |
| Canine | | | | | | |
| 2 mm below CEJ | 0.90 [0.20, 1.40] | 0.90 [0.10, 1.90] | 0.50 [0.20, 1.30] | .5286 | .0054** | .0163* |
| Mid-root | 0.85 [0.30, 2.90] | 0.60 [0.20, 1.70] | 0.50 [0.30, 1.30] | .0118* | .3011 | .0014** |
| Apex | 5.45 [3.30, 8.40] | 4.75 [2.30, 6.50] | 3.80 [2.30, 6.70] | .0038** | .0336* | <.0001**** |
| First premolar | | | | | | |
| 2 mm below CEJ | 0.65 [0.20, 2.00] | 1.00 [0.20, 1.70] | 0.80 [0.20, 1.80] | .2395 | .2232 | .7192 |
| Mid-root | 1.25 [0.40, 3.60] | 1.05 [0.30, 3.00] | 0.65 [0.30, 2.10] | .6618 | .0029** | .0046** |
| Apex | 5.20 [3.30, 7.30] | 4.70 [2.60, 8.40] | 4.15 [2.70, 5.30] | .1058 | .0125* | <.0001**** |
| Second premolar | | | | | | |
| 2 mm below CEJ | 1.15 [0.50, 2.50] | 1.30 [0.40, 2.40] | 1.25 [0.40, 1.70] | .0926 | .3518 | .2938 |
| Mid-root | 2.55 [0.80, 4.10] | 1.85 [0.40, 4.00] | 1.30 [0.40, 2.20] | .0077** | .0021** | <.0001**** |
| Apex | 6.15 [2.80, 8.40] | 5.70 [3.20, 8.40] | 5.20 [2.90, 6.70] | .2720 | .0220* | .0001**** |
| First molar | | | | | | |
| 2 mm below CEJ | 1.20 [0.50, 2.10] | 1.35 [0.80, 2.00] | 1.30 [0.90, 1.80] | .1824 | .3371 | .5159 |
| Mid-root | 3.20 [0.70, 5.50] | 2.50 [1.20, 6.40] | 1.90 [1.00, 3.60] | .0735 | .0451* | <.0001**** |
| Apex | 7.30 [1.40, 8.50] | 7.10 [3.80, 9.40] | 6.45 [4.60, 8.70] | .7119 | .1033 | .0324* |
| Second Molar | | | | | | |
| 2 mm below CEJ | 1.90 [0.90, 4.50] | 1.75 [0.90, 2.70] | 1.60 [1.30, 3.40] | .1610 | .8107 | .2231 |
| Mid-root | 7.40 [2.90, 9.60] | 6.55 [2.30, 11.10] | 6.55 [4.00, 10.30] | .0492* | .8648 | .0217* |
| Apex | 10.60 [6.50, 11.60] | 10.40 [6.00, 13.70] | 9.60 [7.30, 13.10] | .8741 | .5173 | .0855 |

^a CEJ indicates cemento-enamel junction; H, high angle; L, low angle; and N, normal angle.

* $P \leq .05$; ** $P \leq .01$; **** $P \leq .0001$.

premolar regions and the mid-root level of the first molar region (Figure 4).

The thinnest lingual cortical bone (Figure 5, Table 5) was found at 2 mm below the CEJ level of the canines in the high-angle group (0.90 mm [0.50 mm, 1.40 mm]). Statistically significant differences existed among different vertical pattern groups in the canine region at all three axial levels and the first premolar region at the mid-root and apex levels. Pearson correlation coefficient analysis further revealed that statistically negative correlations were detected between the SN-MP angle and lingual alveolar bone thickness at the canine and first premolar regions (Figure 6).

DISCUSSION

The current study demonstrated that, overall, the canine to first molar teeth are located more toward the buccal side of the alveolar ridge and the second molar is located more toward the lingual side of the alveolar ridge. This was consistent with the mandibular anatomic structure, with a deep lingual concavity in the mandible under the second molar¹⁴ and an oblique ridge on the buccal of the second molar.¹⁵

The data showed that the canine region had the thinnest buccal alveolar bone, especially in high-angle subjects. It is worth noting that the buccal alveolar bone thickness at 2 mm below the CEJ and mid-root levels of the canines were all within 0.9 mm

for all three vertical pattern groups. Thus, maintaining mandibular intercanine width should be one of the key treatment objectives while planning orthodontic treatment, especially for patients with a high-angle skeletal pattern. This is consistent with previous publications that stated that the lower intercanine width has been considered to be almost unalterable.^{16,17}

In addition, thin buccal alveolar bone in the range of 1.2 mm was also detected at 2 mm below the CEJ and mid-root levels of the first premolar region. When focusing on the high-angle group, the buccal alveolar bone of the first premolar region was limited to 0.8 mm. Thus, excessive dental expansion should also be avoided in the mandibular first premolar region.

There were several limitations of the current study that should be taken into consideration when interpreting the clinical relevance of the data. First, 3D imaging provides significant advantages over conventional two-dimensional radiographs in the evaluation of bony morphology and size. Timock et al. reported that CBCT can quantitatively assess buccal bone thickness and height with high precision and accuracy.¹⁸ However, a key factor influencing in vivo spatial resolution (the minimum distance needed to distinguish between two objects) is partial volume averaging,^{6,19,20} and thin bone is especially susceptible to it.^{19,21} In this study, a thin layer of alveolar bone with a thickness near or below the voxel size

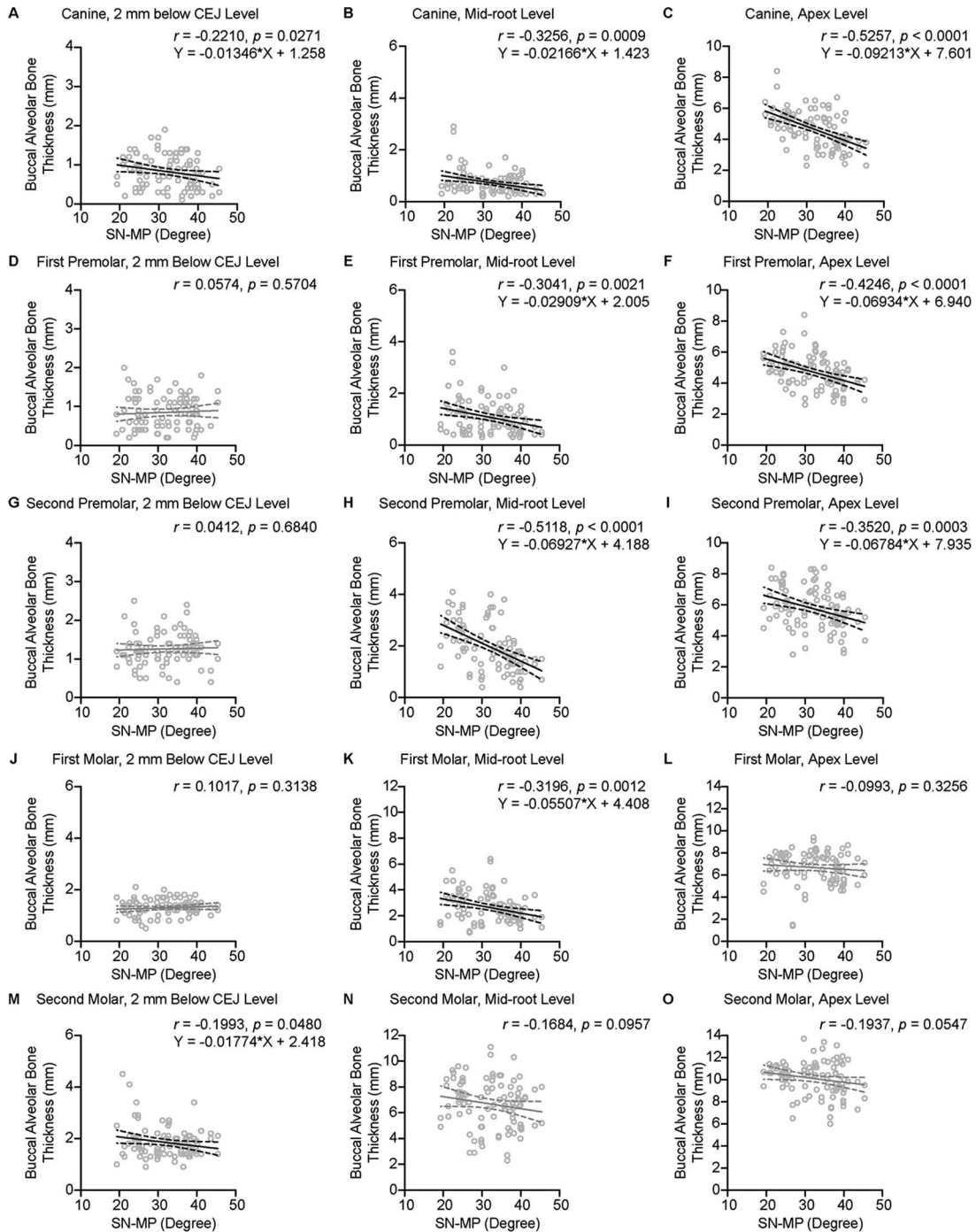


Figure 4. The correlation between sella-nasion–mandibular plane (SN-MP) angle and buccal alveolar bone thickness of mandibular teeth. The correlation between SN-MP angle and buccal alveolar bone thickness of (A–C) canine, (D–F) first premolar, (G–I) second premolar, (J–L) first molar, and (M–O) second molar. The middle straight line represents the linear regression between two parameters. The two curved dashed lines above and below the straight line represent the 95% confidence interval of the regression analysis. The lines are marked in black if the *P* value of correlation analysis is less than .05. The lines are marked in gray if the *P* value of correlation analysis is larger than .05. For the location where a statistically significant correlation was detected, the equation of linear regression analysis is presented: X indicates SN-MP angle in degrees and Y indicates buccal alveolar bone thickness in millimeters. CEJ indicates cemento-enamel junction; SN-MP, sella-nasion–mandibular plane.

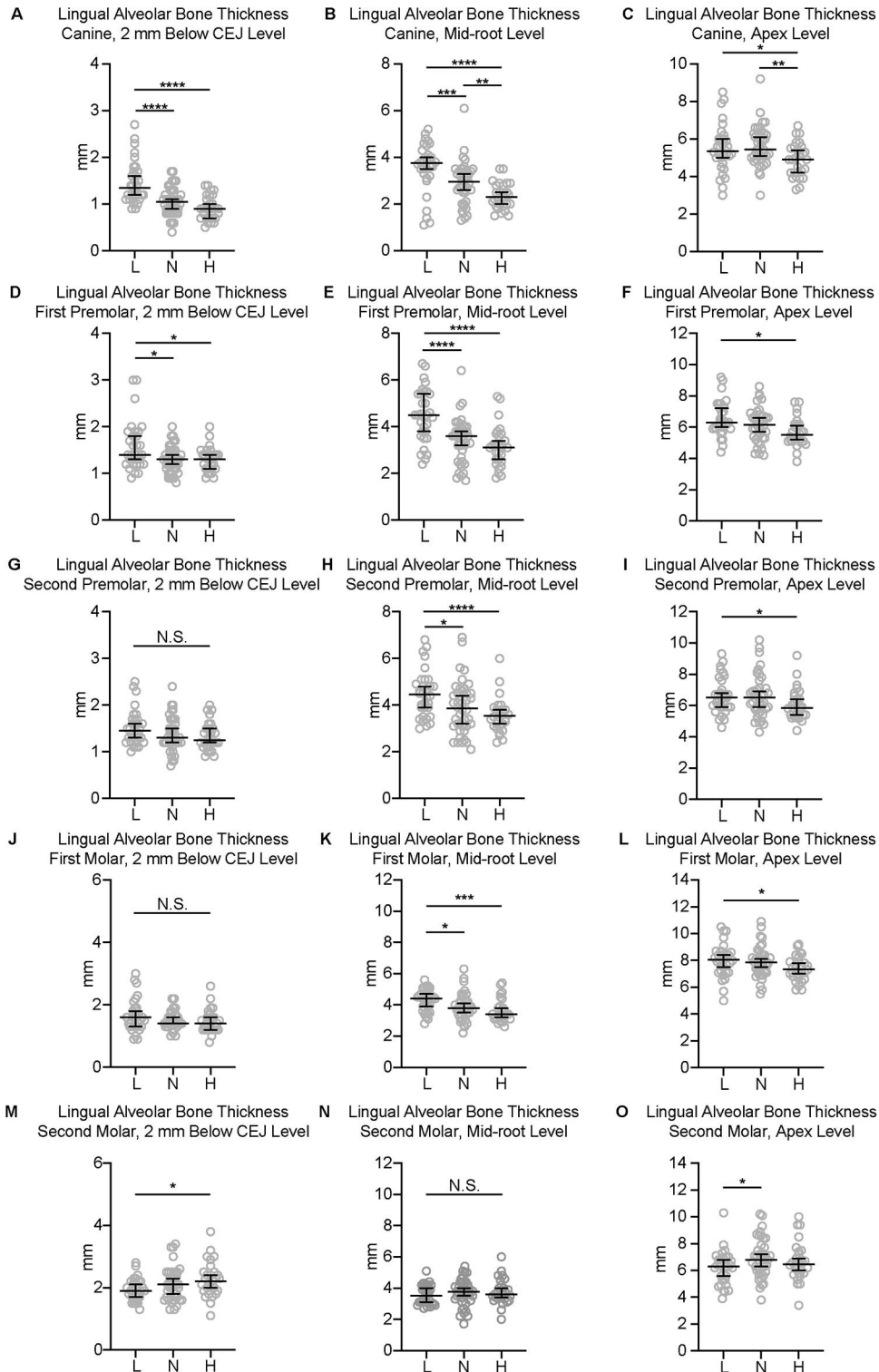


Figure 5. Lingual alveolar bone thickness of mandibular teeth. Lingual alveolar bone thickness of (A–C) canine, (D–F) first premolar, (G–I) second premolar, (J–L) first molar, and (M–O) second molar. Data are presented as raw data overlapped with median ± 95% confidence interval. * $P \leq .05$; ** $P \leq .01$; *** $P \leq .001$; **** $P \leq .0001$. CEJ indicates cemento-enamel junction; H, high angle; L, low angle; N, normal angle; and N.S., not statistically significant.

Table 5. Lingual Alveolar Bone Thickness of Mandibular Canine to Second Molar^a

| | Lingual Alveolar Bone Thickness, Median [Minimum, Maximum], mm | | | P Value of Mann-Whitney U-Test | | |
|------------------------|---|--------------------|--------------------|--------------------------------|---------|------------|
| | L | N | H | L vs N | N vs H | L vs H |
| Canine | | | | | | |
| 2 mm below CEJ | 1.35 [0.90, 2.70] | 1.05 [0.40, 1.70] | 0.90 [0.50, 1.40] | <.0001**** | .0628 | <.0001**** |
| Mid-root | 3.75 [1.10, 5.20] | 2.95 [1.30, 6.10] | 2.30 [1.50, 3.50] | .0002*** | .0058** | <.0001**** |
| Apex | 5.35 [3.00, 8.50] | 5.45 [3.00, 9.20] | 4.90 [3.30, 6.70] | .6099 | .0049** | .0484* |
| First premolar | | | | | | |
| 2 mm below CEJ | 1.40 [0.90, 3.00] | 1.30 [0.80, 2.00] | 1.30 [0.90, 2.00] | .0144* | .9033 | .0344* |
| Mid-root | 4.50 [2.40, 6.70] | 3.60 [1.70, 6.40] | 3.10 [1.80, 5.30] | <.0001**** | .1426 | <.0001**** |
| Apex | 6.30 [4.40, 9.20] | 6.15 [4.20, 8.60] | 5.50 [3.80, 7.60] | .1702 | .0548 | .0012** |
| Second premolar | | | | | | |
| 2 mm below CEJ | 1.45 [1.00, 2.50] | 1.30 [0.70, 2.40] | 1.25 [0.90, 2.00] | .1576 | .6196 | .0545 |
| Mid-root | 4.45 [3.00, 6.80] | 3.85 [2.10, 6.90] | 3.55 [2.40, 6.00] | .0221* | .2079 | .0001**** |
| Apex | 6.50 [4.60, 9.30] | 6.50 [4.30, 10.20] | 5.85 [4.40, 9.20] | .8370 | .0718 | .0287* |
| First molar | | | | | | |
| 2 mm below CEJ | 1.60 [0.90, 3.00] | 1.40 [1.00, 2.20] | 1.40 [0.80, 2.60] | .4512 | .3144 | .1191 |
| Mid-root | 4.40 [2.80, 5.60] | 3.80 [2.20, 6.30] | 3.40 [2.60, 5.40] | .0164* | .0880 | .0006*** |
| Apex | 8.05 [5.00, 10.50] | 7.85 [5.50, 10.90] | 7.35 [5.80, 9.20] | .4966 | .0606 | .0232* |
| Second molar | | | | | | |
| 2 mm below CEJ | 1.90 [1.30, 2.80] | 2.10 [1.30, 3.40] | 2.20 [1.10, 3.80] | .2270 | .2507 | .0130* |
| Mid-root | 3.50 [2.70, 5.10] | 3.75 [1.70, 5.40] | 3.60 [2.00, 6.00] | .3911 | .8404 | .3275 |
| Apex | 6.30 [3.90, 10.30] | 6.80 [3.80, 10.20] | 6.45 [3.40, 10.00] | .0279* | .4292 | .2364 |

^a CEJ indicates cemento-enamel junction; H, high angle; L, low angle; and N, normal angle.

* $P \leq .05$; ** $P \leq .01$; *** $P \leq .001$; **** $P \leq .0001$.

(0.4 mm) can become indistinguishable from the adjacent periodontal ligament and not considered bone when making the alveolar bone thickness measurements.^{21,22} Thus, the current study may have underestimated the alveolar bone thickness.

Second, as the primary goal of the current project was to evaluate the potential alveolar bone boundary in the mandibular posterior region for patients who needed comprehensive orthodontic treatment, patients who had a full permanent dentition (except the third molars) with second molars fully erupted and in occlusion and who were ready to start orthodontic treatment were chosen, which led to the age range selection in our study design. According to the recent publication by Hardin et al., craniofacial growth can continue up to 24 years of age in some individuals.²³ Thus, the alveolar bone morphology of the subjects younger than 24 years of age may continue to change during late growth, and pooling the patients at different ages together may have overlooked the influence of late craniofacial growth on the alveolar bone thickness, although there is controversy regarding the association of alveolar bone thickness with age.²⁴ In the current study, patients of varying age ranges were relatively evenly distributed among the three groups. However, future studies evaluating alveolar bone thickness differences among different age groups, as well as the differences in treatment responses on the alveolar bone thickness change from a similar amount of dental

expansion on patients in different age groups, would hold great clinical significance.

Third, the current study did not compare the sex-based differences and only included Asian subjects. It has been reported that sex is one of the factors that can potentially affect alveolar bone thickness.²⁴ Thus, further studies should evaluate the correlation between skeletal vertical pattern and alveolar bone thickness in males and females.

CONCLUSIONS

- Buccolingual movement of the mandibular teeth, especially in the canine and first premolar regions, should be limited in order to confine teeth within the dimensions of the alveolus.
- There is a statistically significant negative correlation between a vertical facial pattern (SN-MP angle) and mandibular posterior buccal and lingual alveolar thickness. Clinical caution should be taken when treating high-angle patients.

DISCLOSURES

This study was supported by an American Association of Orthodontists Full-Time Faculty Fellowship Award (for C.L.), University of Pennsylvania School of Dental Medicine Joseph and Josephine Rabinowitz Award for Excellence in Research (for C.L.), and the J. Henry O'Hern Jr. Pilot Grant from the Department of Orthodontics, University of Pennsylvania School of Dental Medicine (for C.L.).

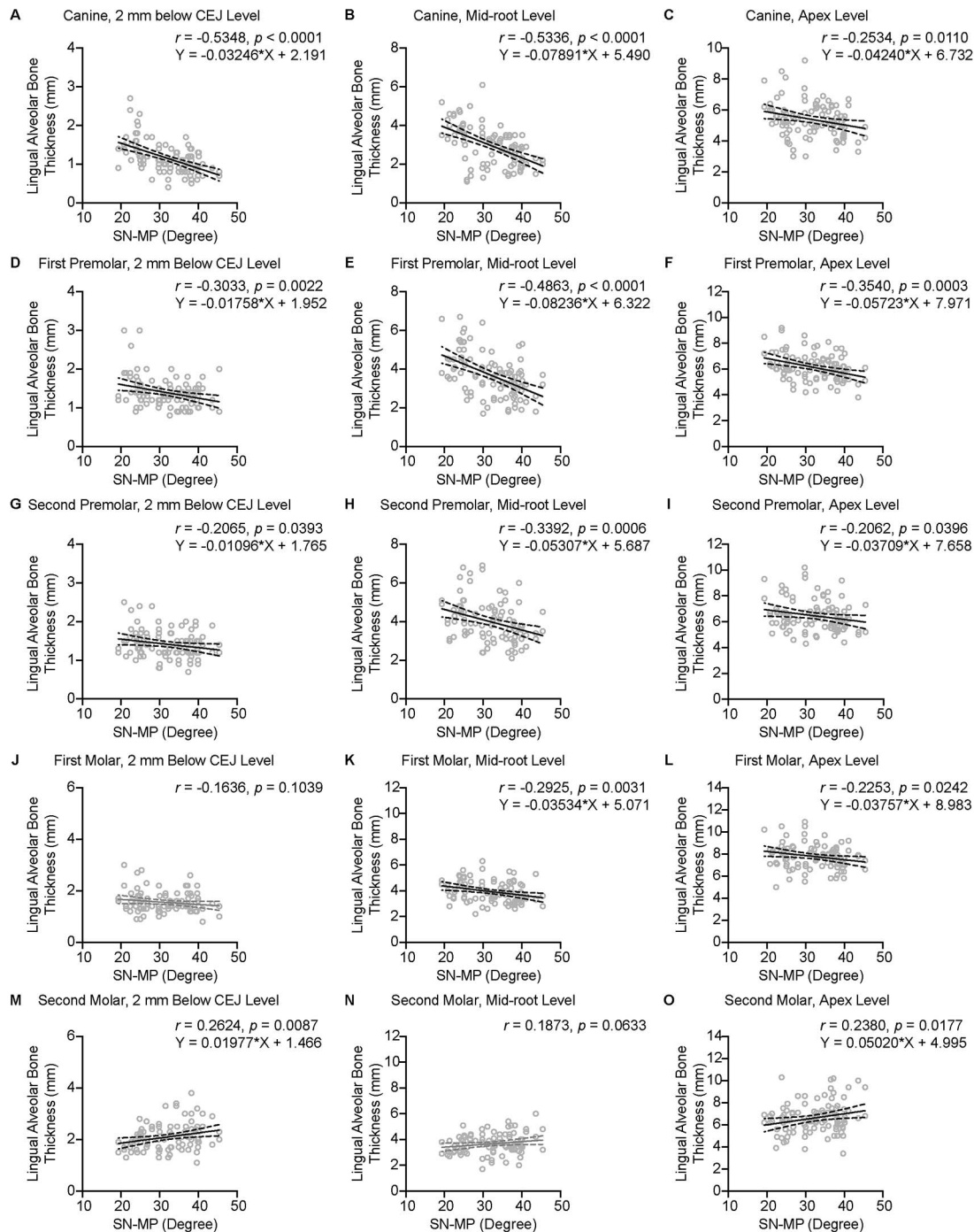


Figure 6. The correlation between SN-MP angle and lingual alveolar bone thickness of mandibular teeth. The correlation between SN-MP angle and lingual alveolar bone thickness of (A–C) canine, (D–F) first premolar, (G–I) second premolar, (J–L) first molar, and (M–O) second molar. The middle straight line represents the linear regression between two parameters. The two curved dashed lines above and below the straight line represent the 95% confidence interval of the regression analysis. The lines are marked in black if the *P* value of correlation analysis is less than .05. The lines are marked in gray if the *P* value of correlation analysis is larger than .05. For the location where a statistically significant correlation was detected, the equation of linear regression analysis is presented: X indicates SN-MP angle in degrees and Y indicates lingual alveolar bone thickness in millimeters. CEJ indicates cemento-enamel junction; SN-MP, sella-nasion–mandibular plane.

REFERENCES

1. Cortellini P, Bissada NF. Mucogingival conditions in the natural dentition: narrative review, case definitions, and diagnostic considerations. *J Periodontol*. 2018;89(suppl 1):S204–S213.
2. Wennström JL. Mucogingival considerations in orthodontic treatment. *Semin Orthod*. 1996;2(1):46–54.
3. Glass TR, Tremont T, Martin CA, Ngan PW. A CBCT evaluation of root position in bone, long axis inclination and relationship to the WALA Ridge. *Semin Orthod*. 2019;25(1):24–35.
4. Allahham DO, Kotsailidi EA, Barmak AB, Rossouw PE, El-Bialy T, Michelogiannakis D. Association between nonextraction clear aligner therapy and alveolar bone dehiscences and fenestrations in adults with mild-to-moderate crowding. *Am J Orthod Dentofacial Orthop*. 2023;163(1):22–32, e24.
5. Gracco A, Luca L, Bongiorno MC, Siciliani G. Computed tomography evaluation of mandibular incisor bony support in untreated patients. *Am J Orthod Dentofacial Orthop*. 2010;138(2):179–187.
6. Sadek MM, Sabet NE, Hassan IT. Alveolar bone mapping in subjects with different vertical facial dimensions. *Eur J Orthod*. 2015;37(2):194–201.
7. Lee S, Hwang S, Jang W, Choi YJ, Chung CJ, Kim KH. Assessment of lower incisor alveolar bone width using cone-beam computed tomography images in skeletal Class III adults of different vertical patterns. *Korean J Orthod*. 2018;48(6):349–356.
8. Casanova-Sarmiento JA, Arriola-Guillen LE, Ruiz-Mora GA, Rodriguez-Cardenas YA, Aliaga-Del Castillo A. Comparison of anterior mandibular alveolar thickness and height in young adults with different sagittal and vertical skeletal relationships: a CBCT Study. *Int Orthod*. 2020;18(1):79–88.
9. Wang J, Zou M, Syverson A, Zheng Z, Li C. Maxillary sinus dimensions in Skeletal Class I Chinese population with different vertical skeletal patterns: a cone-beam computed tomography study. *Diagnostics (Basel)*. 2022;12(12):3144.
10. Cao L, Li J, Yang C, Hu B, Zhang X, Sun J. High-efficiency treatment with the use of traditional anchorage control for a patient with Class II malocclusion and severe overjet. *Am J Orthod Dentofacial Orthop*. 2019;155(3):411–420.
11. Li X, Wang H, Li S, Bai Y. Treatment of a Class II Division 1 malocclusion with the combination of a myofunctional trainer and fixed appliances. *Am J Orthod Dentofacial Orthop*. 2019;156(4):545–554.
12. Song G, Chen H, Xu T. Nonsurgical treatment of Brodie bite assisted by 3-dimensional planning and assessment. *Am J Orthod Dentofacial Orthop*. 2018;154(3):421–432.
13. Sawilowsky SS. New effect size rules of thumb. *J Mod Appl Stat Methods*. 2009;8(2):26.
14. Tan WY, Ng JZL, Ajit Bapat R, Vijaykumar Chaubal T, Kishor Kanneppedy S. Evaluation of anatomic variations of mandibular lingual concavities from cone beam computed tomography scans in a Malaysian population. *J Prosthet Dent*. 2021;125(5):766.e1–766.e8.
15. Chang C, Liu SS, Roberts WE. Primary failure rate for 1680 extra-alveolar mandibular buccal shelf mini-screws placed in movable mucosa or attached gingiva. *Angle Orthod*. 2015;85(6):905–910.
16. Little RM. Stability and relapse of dental arch alignment. *British J Orthod*. 1990;17(3):235–241.
17. Rossouw PE, Preston CB, Lombard CJ, Truter JW. A longitudinal evaluation of the anterior border of the dentition. *Am J Orthod Dentofacial Orthop*. 1993;104(2):146–152.
18. Timock AM, Cook V, McDonald T, et al. Accuracy and reliability of buccal bone height and thickness measurements from cone-beam computed tomography imaging. *Am J Orthod Dentofacial Orthop*. 2011;140(5):734–744.
19. Molen AD. Considerations in the use of cone-beam computed tomography for buccal bone measurements. *Am J Orthod Dentofacial Orthop*. 2010;137(4 suppl):S130–S135.
20. Swasty D, Lee J, Huang JC, et al. Cross-sectional human mandibular morphology as assessed in vivo by cone-beam computed tomography in patients with different vertical facial dimensions. *Am J Orthod Dentofacial Orthop*. 2011;139(4 suppl):e377–e389.
21. Sun Z, Smith T, Kortam S, Kim DG, Tee BC, Fields H. Effect of bone thickness on alveolar bone-height measurements from cone-beam computed tomography images. *Am J Orthod Dentofacial Orthop*. 2011;139(2):e117–e127.
22. Garlock DT, Buschang PH, Araujo EA, Behrents RG, Kim KB. Evaluation of marginal alveolar bone in the anterior mandible with pretreatment and posttreatment computed tomography in nonextraction patients. *Am J Orthod Dentofacial Orthop*. 2016;149(2):192–201.
23. Hardin AM, Knigge RP, Oh HS, et al. Estimating craniofacial growth cessation: comparison of asymptote- and rate-based methods. *Cleft Palate Craniofac J*. 2022;59(2):230–238.
24. Shafizadeh M, Tehranchi A, Shirvani A, Motamedian SR. Alveolar bone thickness overlying healthy maxillary and mandibular teeth: a systematic review and meta-analysis. *Int Orthod*. 2021;19(3):389–405.

Copyright of Angle Orthodontist is the property of Angle Orthodontist Research Education Foundation and its content may not be copied or emailed to multiple sites or posted to a listserv without the copyright holder's express written permission. However, users may print, download, or email articles for individual use.